

Resonant Enhancement of Inelastic Light Scattering in the Fractional Quantum Hall Regime at $\nu = 1/3$

C.F. Hirjibehedin,^{1,2} Irene Dujovne,^{3,2} I. Bar-Joseph,⁴ A. Pinczuk,^{1,2,3} B.S. Dennis,² L.N. Pfeiffer,² and K.W. West²

¹*Department of Physics, Columbia University, New York, NY 10027*

²*Bell Labs, Lucent Technologies, Murray Hill, NJ 07974*

³*Department of Appl. Physics and Appl. Mathematics, Columbia University, New York, NY 10027*

⁴*Department of Condensed Matter Physics, The Weizmann Institute of Science, Rehovot 76100, Israel*

(Dated: June 25, 2003)

Strong resonant enhancements of inelastic light scattering from the long wavelength inter-Landau level magnetoplasmon and the intra-Landau level spin wave excitations are seen for the fractional quantum Hall state at $\nu = 1/3$. The energies of the sharp peaks (FWHM $\lesssim 0.2\text{meV}$) in the profiles of resonant enhancement of inelastic light scattering intensities coincide with the energies of photoluminescence bands assigned to negatively charged exciton recombination. To interpret the observed enhancement profiles, we propose three-step light scattering mechanisms in which the intermediate resonant transitions are to states with charged excitonic excitations.

PACS numbers: 73.20.Mf, 73.43.Lp, 71.35.Ji

Inelastic light scattering is a key method for the study of collective excitation modes in quantum Hall (QH) liquids [1, 2, 3, 4, 5, 6, 7, 8, 9, 10]. Resonant enhancement of the scattering cross-section is here crucial because the non-resonant scattering intensity in 2D electron systems is too small to be observable [1, 11, 12, 13, 14, 15]. The enhancement of the scattering cross-section also plays a role in degenerate four-wave mixing [16] and coherent optical oscillation [17] studies. In the presence of weak residual disorder, breakdown of wavevector conservation in light scattering processes offers direct access to critical points in the dispersions of charge and spin excitations of QH liquids [1, 2, 3, 4, 7, 8, 18]. However, only brief attention has been given to the resonance profiles and the details of the underlying enhancement mechanisms of the observed collective excitations.

Here we present resonance enhancement profiles in the fractional QH (FQH) regime and discuss their implications, particularly in relation to optical transitions that have been the focus of much recent work [19, 20, 21, 22, 23, 24, 25, 26, 27, 28, 29, 30, 31, 32, 33, 34]. We focus our attention on the resonance enhancement profiles for inelastic light scattering when the electron system is in the major FQH state with $\nu = 1/3$, where $\nu = nhc/eB$ is the Landau level filling factor for areal density n and perpendicular magnetic field B . We consider the enhancement profiles of the inter-Landau level magnetoplasmon (MP) mode at the cyclotron energy ω_c and the intra-Landau level spin wave (SW) at the Zeeman energy E_z . In the MP mode only the electron Landau level index changes and in the SW mode there is only reversal in spin orientation of electrons and/or quasiparticles of quantum liquids. Both collective modes occur at $q \rightarrow 0$, so that the impact of breakdown of wavevector conservation is ignored in a lowest order description.

We find strong enhancement of the light scattering intensity within a small range of incoming and outgoing

photon energies. These enhancements coincide with optical transitions assigned to recombination of negatively charged excitons (X^-) [22, 25, 29, 30]. The large resonance enhancements reported here enable light scattering studies at the very low light power densities required to achieve temperatures in the milliKelvin regime under experimental conditions [35, 36, 37]. In a qualitative interpretation, we propose three-step light scattering mechanisms that interpret the resonance enhancements with intermediate transitions to states with X^- excitations [1, 11, 12, 13, 14, 15].

The links between resonant enhancements of light scattering and the X^- excitations provides new venues for the study of the properties of X^- . Studies of resonant enhancement of light scattering by modes seen due to breakdown of wavevector conservation in the FQH regime [8, 36] will be the subject of future work. Well-defined polarization selection rules, which are seen in some resonances, also offer new venues for exploring the properties of X^- transitions.

The 2D electron systems studied here are formed in 250Å- and 330Å-wide asymmetrically doped GaAs single quantum wells, referred to as samples A and B. The electron densities for the two samples are $8.5 \times 10^{10}\text{cm}^{-2}$ and $5.4 \times 10^{10}\text{cm}^{-2}$ and the low temperature mobilities are $3.0 \times 10^6\text{cm}^2/\text{Vs}$ and $7.2 \times 10^6\text{cm}^2/\text{Vs}$, respectively. As shown in the schematic in Fig. 1, the samples are mounted on the cold finger of a dilution refrigerator with a base temperature of 50mK. This is inserted into the cold bore of a 17T superconducting magnet. The samples are mounted with the normal to the surface at an angle θ from the magnetic field, making the component of the field perpendicular to the 2D electron layer $B = B_T \cos\theta$ for a total applied field B_T .

As shown in the schematic in Fig. 1, light scattering measurements are performed through windows for direct optical access. The energy of the linearly polar-

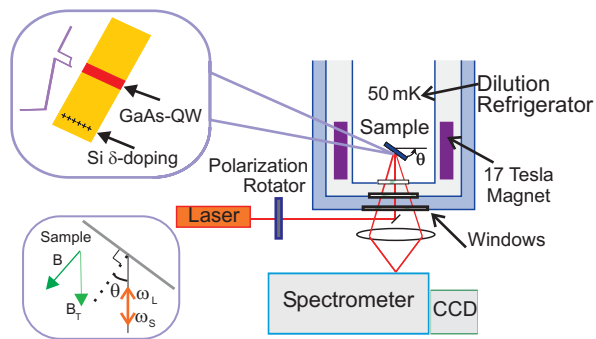


FIG. 1: A schematic of the experimental setup and measurement configuration. Linearly polarized light from a tunable laser is passed through a polarization rotator and directed onto the sample through windows. The scattered light is focused into a spectrometer and the dispersed light is detected by a CCD. The upper inset shows the sample design and a sketch of the conduction band. The lower inset shows the backscattering geometry.

ized incident photons is tuned close to the fundamental optical gap of the GaAs well and the power density is kept below 10^{-4}W/cm^2 . The samples are measured in a backscattering geometry, making an angle θ between the incident/scattered photons and the normal to the sample surface. The wavevector transferred from the photons to the 2D system is $k = (2\omega_L/c)\sin\theta$. For typical measurement geometries, $\theta < 60^\circ$ so that $k \leq 1.5 \times 10^5 \text{cm}^{-1} \ll 1/l_0$, where $l_0 = (\hbar c/eB)^{1/2}$ is the magnetic length. Scattered light is dispersed by a Spex 1404 double spectrometer with holographic master gratings that reduce the stray light and provide a resolution as small as $20 \mu\text{eV}$. The response of the spectrometer is linearly polarized, so that spectra can be taken with the linear polarization of the incident photons parallel (polarized) or perpendicular (depolarized) to the detected scattered photons' polarization.

Figure 2a shows spectra at $\nu = 1/3$. In these spectra, the collective excitation energy is measured as a shift below the laser energy ω_L . The sharp peak labelled ω_c , found at a constant shift of 17.2meV for various ω_L , is inelastic light scattering from the long wavelength (i.e. at wavevector $q \rightarrow 0$) MP. This mode is fixed by Kohn's theorem at the cyclotron energy $\omega_c = eB/m^*c$. Two additional features are also seen at shifts from the laser that depend on laser photon energy. These are more easily understood in Fig. 2b, where the spectra are plotted on an absolute energy scale. The features at 1523.7meV and 1524.3meV are luminescence from optical transitions identified as the singlet (S_1) and bright triplet (T_B) X^- recombination [22, 25, 29, 30]. From Fig. 2, it is clear that for the excitation at ω_c the light scattering process is resonant when the outgoing photon energy ω_S coincides with the T_B transition.

Overlap of ω_L or ω_S with an X^- transition can cause

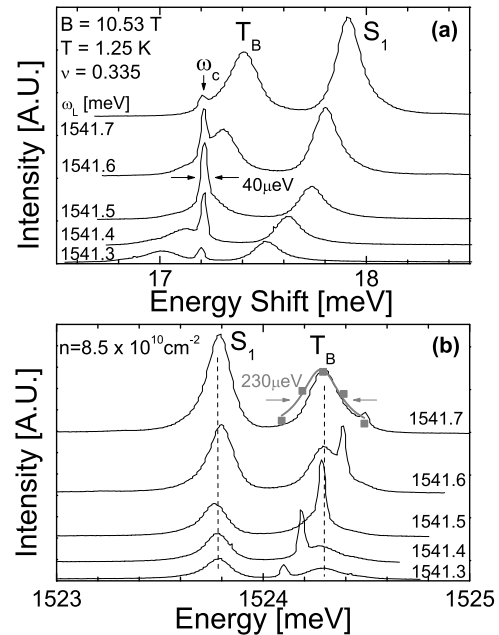


FIG. 2: Spectra at various ω_L for $\nu = 1/3$ in sample A (after Ref [38]), translated vertically for clarity. (a) Spectra are plotted as intensity vs. energy shift below ω_L . The mode at a constant shift of 17.2meV labelled ω_c is light scattering from the MP excitation. (b) The same spectra are plotted as intensity vs. absolute photon energy. The peaks labelled S_1 and T_B are identified as luminescence from X^- excitations, as discussed in the text. Grey dots overlaid on the 1541.7meV spectrum are the intensity of the light scattering from the MP mode vs. ω_S , and the grey line is a fit using Eq. 2.

striking increases in the light scattering intensities by excitation modes of liquids in the FQH regime. We see from Fig. 2a that the intensity of the MP mode in sample A becomes significantly larger when ω_S overlaps T_B . Remarkably, the intensity of the scattered light at the peak of this outgoing resonance can be larger than that of the luminescence. In Fig. 2b we show the resonance enhancement profile for the MP mode as a function of ω_S overlaid on the luminescence. The lineshape of the outgoing resonance profile of light scattering intensity corresponds very closely to that of the T_B luminescence, and both are peaked at 1524.28meV . The T_B luminescence lineshape has a FWHM of 0.17meV , which is narrower than the FWHM of 0.23meV for the resonance profile.

Figure 3a shows light scattering spectra from the long wavelength intra-Landau level spin wave (SW) excitation in sample B. The energy of this mode is fixed by Larmor's Theorem at the Zeeman energy $E_z = g\mu_B B_T$, where g is the Lande g -factor in GaAs and μ_B is the Bohr magneton [6]. The SW is resonant throughout a broad range of ω_L and ω_S . In the results reported here the focus of our current analysis is on the strongest and lowest energy resonance, where the peak intensity is at least a

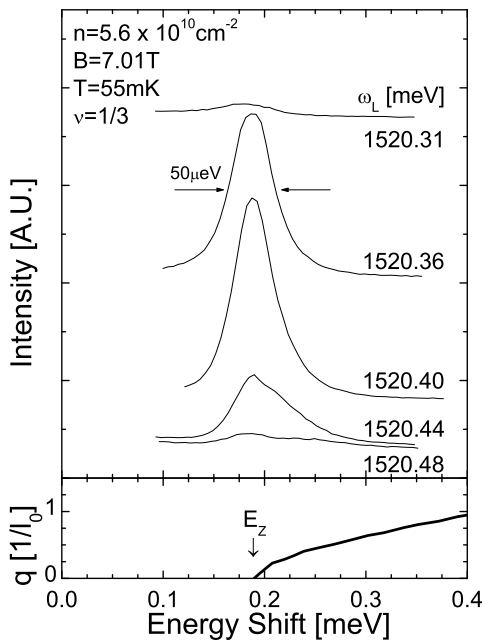


FIG. 3: (a) Spectra at various ω_L for $\nu = 1/3$ in sample B, translated vertically for clarity. Spectra are plotted as intensity vs. energy shift below ω_L . (b) Calculation of SW dispersion [39] including a scaling by a factor of 0.59 to incorporate finite width corrections [8, 37].

factor of two larger than in other resonances. One striking difference between these spectra and those for the ω_c resonance is that no luminescence is seen when ω_L overlaps or is below the energy of the neutral exciton (X) optical recombination energy. It is possible that photoexcited states are unable to relax and then emit if the exciting photon energy is below a certain threshold. This is consistent with our observations that the luminescence appears for higher energy ω_L .

As seen in Fig. 3a, the SW has a relatively narrow $FWHM = 50\mu eV$. However, its lineshape is asymmetric because of an enhanced tail on the high energy side. In Fig. 3b we show the SW dispersion $\omega_{SW} = E_z + \alpha\Delta_{SW}(q)$, where $\Delta_{SW}(q)$ is calculated exactly for finite sized systems [39] and $\alpha = 0.59$ is a constant scaling factor to account for finite width effects [8, 37]. Breakdown of wavevector conservation from residual disorder can activate larger wavevector SW excitations. As seen in Fig. 3b these occur above E_z , causing the observed asymmetry [40].

In Fig. 4, we compare the SW resonance enhancement profile to the luminescence lineshape. Assignment of the two singlet (S_1 and S_2), dark triplet (T_D), and bright triplet (T_B) luminescence features is made based on the arguments presented in Refs. [22, 25, 29, 30]. The S_2 transition has a particularly low intensity, but is more clearly seen in other spectra (not shown). The peak in

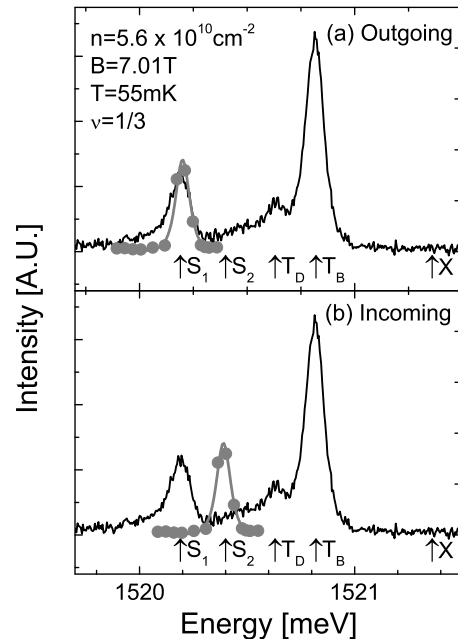


FIG. 4: Luminescence intensity vs. absolute energy for sample B taken with $\omega_L = 1525.02 meV$. Arrows at the bottom of each panel label the transitions to which the features are assigned. The overlaid grey dots are the resonance enhancement profile of the SW vs. (a) ω_S and (b) ω_L . The intensities have been scaled by a constant to match the intensity of the S_1 luminescence.

the resonance profile has a $FWHM < 0.1 meV$, which is slightly sharper than the luminescence linewidths. From Fig. 4a, we find the peak in scattering intensity occurs when ω_S coincides with the feature assigned to the S_1 luminescence transition. The incoming resonance shown in Fig. 4b indicates that the peak also overlaps the feature assigned to the S_2 luminescence.

The simplest mechanism for wavevector conserving light scattering processes that exhibit both incoming and outgoing resonances is a third-order process. The intensity of this process, which is described in the diagram shown in Fig. 5, can be written within time-dependent perturbation theory as [1, 41]

$$I(\omega) \sim \left| \sum_{i,j} \frac{\langle 0 | H_\gamma | j \rangle \langle j | H_{int} | i \rangle \langle i | H_\gamma | 0 \rangle}{(\omega_S - E_j)(\omega_L - E_i)} \right|^2, \quad (1)$$

where the intermediate states $|i\rangle$ and $|j\rangle$ have energies E_i and E_j above the ground state respectively. In the first step, the incoming photon ω_L is annihilated and the system goes from state $|0\rangle$ to an intermediate state $|i\rangle$ via a virtual transition through the electron-photon interaction H_γ . The system then goes from $|i\rangle$ to $|j\rangle$ through the H_{int} interaction between the electrons and the collective excitations of the 2D system. In this second step there is

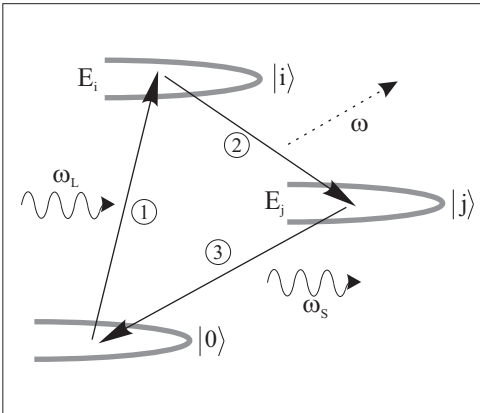


FIG. 5: Diagrammatic representation of third-order resonant light scattering process described by Eq. 1. The numbers indicate the time ordering of the processes.

emission of a collective excitation at ω . In the third and final step, the electron system returns to state $|0\rangle$ with the additional collective excitation at ω and emits a photon at energy $\omega_S = \omega_L - \omega$. The quasiparticle properties of the electron liquids are here incorporated into H_{int} . In the specific case of the SW we note that the excitation is a collective mode associated with spin-reversed transition of composite fermions (CFs) [39, 42]. Here H_{int} must arise from the residual interactions between composite fermions.

The peaks in the resonance profiles shown in Figs. 2 and 4 coincide with luminescence transitions of X^- . From this, we infer that the intermediate states of the third-order light scattering mechanism are excitations of the ground state that can include X^- transitions and a collective excitation. Enhancement of light scattering in the FQH regime is then directly linked to X^- transitions, and their symmetry properties will determine the selection rules.

Light scattering from the MP mode is seen in Fig. 2 to have an outgoing resonance with the T_B state. Assuming there is no double resonance condition (simultaneous incoming and outgoing resonances), the scattering intensity in this range can be written as

$$I(\omega) \sim \frac{1}{(\omega_S - E_{T_B})^2 + \Gamma^2}, \quad (2)$$

where Γ is a broadening of the transition. The best fit of Eq. 2 to the resonance profile of the MP mode with $\Gamma = 0.11\text{meV}$ is shown in Fig. 2. The FWHM is $2\Gamma = 0.22\text{meV}$, which is consistent with the width of the T_B transition as measured by the luminescence linewidth.

From Fig. 4, the SW mode shows an outgoing resonance but no incoming resonance with the S_1 state. Assuming the product of matrix elements in Eq. 1 is the

same under interchange of states i and j , we would expect an incoming and outgoing resonance at close to the same intensity. Because the SW energy at $1/3$ in sample B is close to the spacing of the X^- transitions shown in the luminescence of Fig. 4, it is possible to have a double resonance condition, in which the incoming and outgoing resonances for two states coincide. For the SW resonance shown in Fig. 4, the spacing of the S_1 and S_2 transitions is close to $E_z = 0.19\text{meV}$. The resonance lineshape from Eq. 1 can then be written as

$$I(\omega) \sim \frac{1}{((\omega_S - E_{S_1})^2 + \Gamma^2)((\omega_L - E_{S_2})^2 + \Gamma^2)}, \quad (3)$$

where both levels are assumed to have the same broadening. The best fit of Eq. 3 to the resonance profile of the SW mode with $\Gamma = 0.06\text{meV}$ is shown in Fig. 4. The FWHM of the lineshape is slightly wider than this at 0.08meV . This is sharper than the linewidth of S_1 or S_2 , indicating that the luminescence transition is broadened by additional mechanisms that do not contribute to the light scattering process.

Large resonance enhancements of the light scattering intensities such as those reported here are crucial in the study of FQH liquids. Significant examples are found in recent work that examines the important low-lying excitations that manifest key characteristics of the liquids, as in recent studies between major fractions in the sequence $\nu = p/(2p + 1)$ [10, 36] and FQH states in the sequence $\nu = p/(4p \pm 1)$ [37] for integer p . The excitations measured in these studies typically have low energy ($< 0.5\text{meV}$) and require temperatures reaching below 100mK . Because of the small ($< 1\text{meV}$) spacing between various X^- transitions, double resonances similar to those seen for the SW are possible for many low-energy excitations in the FQH regime. With such resonances, studies can be performed using the very low light power densities required to obtain very low temperatures.

In summary, we find strong resonance enhancement of inelastic light scattering in the FQH state at $\nu = 1/3$. Enhancement profiles of long wavelength MP and SW modes show incoming and outgoing resonances that coincide with X^- optical transitions seen in luminescence. The enhancements are interpreted by three-step light scattering mechanisms in which the intermediate states are excitations of the ground state with X^- excitations.

This work was supported in part by the Nanoscale Science and Engineering Initiative of the National Science Foundation under NSF Award Number CHE-0117752, by a research grant of the W. M. Keck Foundation, and by the Israeli Academy of Science.

[1] A. Pinczuk, J. P. Valladares, D. Heiman, A. C. Gossard, J. H. English, C. W. Tu, L. Pfeiffer, and K. West, Phys.

- Rev. Lett. **61**, 2701 (1988).
- [2] A. Pinczuk, B. S. Dennis, D. Heiman, C. Kallin, L. Brey, C. Tejedor, S. Schmitt-Rink, L. N. Pfeiffer, and K. W. West, Phys. Rev. Lett. **68**, 3623 (1992).
- [3] A. Pinczuk, B. S. Dennis, L. N. Pfeiffer, and K. West, Phys. Rev. Lett. **70**, 3983 (1993).
- [4] H. D. M. Davies, J. C. Harris, J. F. Ryan, and A. J. Turberfield, Phys. Rev. Lett. **78**, 4095 (1997).
- [5] C. Schuller, R. Krahne, G. Biese, C. Steinebach, E. Ulrichs, and D. Heitmann, Phys. Rev. B **56**, 1037 (1997).
- [6] V. Pellegrini, A. Pinczuk, B. S. Dennis, A. S. Plaut, L. N. Pfeiffer, and K. W. West, Science **281**, 799 (1998).
- [7] M. A. Eriksson, A. Pinczuk, B. S. Dennis, L. N. Pfeiffer, and K. W. West, Phys. Rev. Lett. **82**, 2163 (1999).
- [8] M. Kang, A. Pinczuk, B. S. Dennis, L. N. Pfeiffer, and K. W. West, Phys. Rev. Lett. **86**, 2637 (2001).
- [9] L. V. Kulik, I. V. Kukushkin, V. E. Kirpichev, J. H. Smet, K. v. Klitzing, and W. Wegscheider, Phys. Rev. B **63**, 201402 (2001).
- [10] I. Dujovne, C. Hirjibehedin, A. Pinczuk, M. Kang, B. Dennis, L. Pfeiffer, and K. West, Solid State Comm. (2003), to be published, cond-mat/0306179.
- [11] E. Burstein, A. Pinczuk, and S. Buchner, *Physics of Semiconductors 1978* (Institute of Physics, London, 1979).
- [12] E. Burstein, A. Pinczuk, and D. L. Millis, Surf. Sci. **98**, 451 (1980).
- [13] A. Pinczuk, B. S. Dennis, L. N. Pfeiffer, K. W. West, and E. Burstein, Phil. Mag. B **70**, 429 (1994).
- [14] P. M. Platzman and S. He, Phys. Rev. B **49**, 13674 (1994).
- [15] S. Das Sarma and D.-W. Wang, Phys. Rev. Lett. **83**, 816 (1999).
- [16] N. A. Fromer, C. E. Lai, D. S. Chemla, I. E. Perakis, D. Driscoll, and A. C. Gossard, Phys. Rev. Lett. **89**, 067401 (2002).
- [17] J. Bao, L. N. Pfeiffer, K. W. West, and R. Merlin, QELS 2002 Technical Digest **74**, 261 (2002).
- [18] I. K. Marmorosk and S. Das Sarma, Phys. Rev. B **45**, 13396 (1992).
- [19] A. H. MacDonald, E. H. Rezayi, and D. Keller, Phys. Rev. Lett. **68**, 1939 (1992).
- [20] B.-S. Wang, J. L. Birman, and Z.-B. Su, Phys. Rev. Lett. **68**, 1605 (1992).
- [21] V. M. Apalkov and E. I. Rashba, Phys. Rev. B **48**, 18312 (1993).
- [22] K. Kheng, R. T. Cox, M. Y. d'Aubigne, F. Bassani, K. Saminadayar, and S. Tatarenko, Phys. Rev. Lett. **71**, 1752 (1993).
- [23] A. Wojs and P. Hawrylak, Phys. Rev. B **51**, 10880 (1995).
- [24] G. Finkelstein, H. Shtrikman, and I. Bar-Joseph, Phys. Rev. Lett. **74**, 976 (1995).
- [25] A. J. Shields, M. Pepper, M. Y. Simmons, and D. A. Ritchie, Phys. Rev. B **52**, 7841 (1995).
- [26] J. J. Palacios, D. Yoshioka, and A. H. MacDonald, Phys. Rev. B **54**, R2296 (1996).
- [27] D. Gekhtman, E. Cohen, A. Ron, and L. N. Pfeiffer, Phys. Rev. B **56**, 12768 (1997).
- [28] A. Wojs, I. Szlufarska, K. S. Yi, and J. J. Quinn, Phys. Rev. B **60**, 11273 (1999).
- [29] A. Wojs, J. J. Quinn, and P. Hawrylak, Phys. Rev. B **62**, 4630 (2000).
- [30] G. Yusa, H. Shtrikman, and I. Bar-Joseph, Phys. Rev. Lett. **87**, 216402 (2001).
- [31] C. Schuller, K. Broocks, C. Heyn, and D. Heitmann, Phys. Rev. B **65**, 081301 (2001).
- [32] I. Szlufarska, A. Wojs, and J. J. Quinn, Phys. Rev. B **63**, 085305 (2001).
- [33] H. A. Nickel, T. M. Yeo, A. B. Dzyubenko, B. D. McCombe, A. Petrou, A. Y. Sivachenko, W. Schaff, and V. Umansky, Phys. Rev. Lett. **88**, 056801 (2002).
- [34] K.-B. Broocks, P. Schroter, D. Heitmann, C. Heyn, C. Schuller, M. Bichler, and W. Wegscheider, Phys. Rev. B **66**, 041309 (2002).
- [35] M. Kang, A. Pinczuk, B. S. Dennis, M. A. Eriksson, L. N. Pfeiffer, and K. W. West, Phys. Rev. Lett. **84**, 546 (2000).
- [36] I. Dujovne, A. Pinczuk, M. Kang, B. S. Dennis, L. N. Pfeiffer, and K. W. West, Phys. Rev. Lett. **90**, 036803 (2003).
- [37] C. F. Hirjibehedin, A. Pinczuk, B. S. Dennis, L. N. Pfeiffer, and K. W. West, cond-mat/0306152 (2003).
- [38] A. Pinczuk, B. S. Dennis, L. N. Pfeiffer, and K. W. West, Semicond. Sci. Technol. **9**, 1865 (1994).
- [39] T. Nakajima and H. Aoki, Phys. Rev. Lett. **73**, 3568 (1994).
- [40] A. Pinczuk, B. S. Dennis, L. N. Pfeiffer, and K. W. West, Physica B **249**, 40 (1998).
- [41] G. Danan, A. Pinczuk, J. P. Valladares, L. N. Pfeiffer, K. W. West, and C. W. Tu, Phys. Rev. B **39**, 5512 (1989).
- [42] S. S. Mandal and J. K. Jain, Phys. Rev. B **64**, 125310 (2001).